

Folded Graph Signals: Sensing with Unlimited Dynamic Range

Feng Ji, Pratibha, and Wee Peng Tay, *Senior Member, IEEE*

Abstract

Self-reset analog-to-digital converters (ADCs) are used to sample high dynamic range signals resulting in modulo-operation based folded signal samples. We consider the case where each vertex of a graph (e.g., sensors in a network) is equipped with a self-reset ADC and senses a time series. Graph sampling allows the graph time series to be represented by the signals at a subset of sampled vertices and time instances. We investigate the problem of recovering bandlimited continuous-time graph signals from folded signal samples. We derive sufficient conditions to achieve successful recovery of the graph signal from the folded signal samples, which can be achieved via integer programming. To resolve the scalability issue of integer programming, we propose a sparse optimization recovery method for graph signals satisfying certain technical conditions. Such an approach requires a novel graph sampling scheme that selects vertices with small signal variation. The proposed algorithm exploits the inherent relationship among the graph vertices in both the vertex and time domains to recover the graph signal. Simulations and experiments on images validate the feasibility of our proposed approach.

Index Terms

Graph sampling, graph signal recovery, folded samples, high dynamic range, unlimited sensing

I. INTRODUCTION

Graph signal processing is an emerging field that studies multidimensional signals embedded in a graph representing the inherent relationship among the different components of the signals [1]. Graph signal processing has attracted increased attention as it allows us to capture complex

This work was supported in part by the Singapore Ministry of Education Academic Research Fund Tier 2 grant MOE2018-T2-2-019 and by A*STAR under its RIE2020 Advanced Manufacturing and Engineering (AME) Industry Alignment Fund – Pre Positioning (IAF-PP) (Grant No. A19D6a0053).

The authors are with the School of Electrical and Electronic Engineering, Nanyang Technological University, 639798, Singapore (e-mail: jifeng@ntu.edu.sg, pratibha001@e.ntu.edu.sg, wptay@ntu.edu.sg).

correlations in many practical problems. It has been applied to various problems consisting of signal recovery, prediction, and anomaly detection [1]–[9]. Recently, much work has been devoted to graph sampling, which studies the recovery of entire graph signal using observations at only some of the graph vertices [10]–[16].

Analog-to-digital converters (ADCs) are used to sample and digitize continuous signals. The Nyquist-Shannon rate is the minimum sampling rate that guarantees perfect recovery of a bandlimited signal from its signal samples [17]. To overcome the problem of signal clipping that occurs during sampling of high dynamic range signals, self-reset ADCs are used to sample modulo-operated signal values, which are called folded samples [18]–[23]. Suppose $[0, \lambda]$ is the maximum amplitude range the ADC can capture. A signal x and its folded version $0 \leq p < \lambda$ (as illustrated in Fig. 1) are related by the following equation analogous to modulo arithmetic:

$$x = \lambda z + p, \quad (1)$$

where $z \in \mathbb{Z}$ is the largest integer not more than x/λ . We call z the folding number.

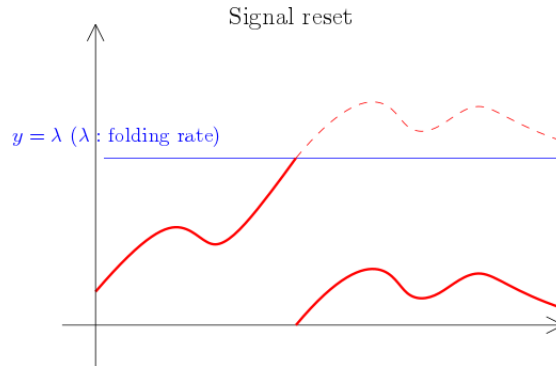


Fig. 1. Signal reset with folding rate λ results a folding signal depicted by the discontinuous solid red curve.

We want to recover the original signal x from the folded signal p without knowledge of the folding number z . In this context, the authors in [21] introduced the concept of unlimited sampling, where a sufficient condition was derived for the recovery of bandlimited signals from the folded samples. They showed that using a sampling rate e (Euler's number) times that of the Nyquist-Shannon rate is sufficient to recover a signal from its folded samples. An earlier related work is [24]. Both papers propose folded signal recovery based on the method of finite-difference and its higher order version. This approach encounters the difficulty when applied to graph signals, as there is no analogous operators on sampled subgraphs. The paper [25]

proposed the notion of one-bit unlimited sampling to overcome the dynamic range limitations of a conventional one-bit quantizer. In [26], the authors developed a generalized approximate message passing algorithm for the reconstruction of discrete-time sparse signals with noise. The reference [27] studied the denoising problem of a smooth function on $[0, 1]$ at discrete sampled points, while observing modulo 1 samples. In [22], the authors considered folded signal recovery where the original signal are annihilated by certain wavelet transforms, in particular, polynomial signals. All the above mentioned works are taking signals from a 1D channel. The authors in [28] investigated modulo sampling based hardware implementation and quantization. Signals are recovered from the folded samples together with complete signals from the past. The signals considered in this paper can be vector valued, however, no graph structured signals are considered. On the other hand, there are also considerable effects on the hardware side to build self-reset counter CMOS such as [29], [30].

The signals observed in many applications can be modeled as graph signals, for example, photo and microscopic images [30], and readings from sensor networks. This motivates us to study signal recovery from folded versions in the context of graph signals. Different from most of the other related works on folded signals described above that considers only a single continuous-time signal, we consider the problem of recovery of a *continuous-time graph signal* in which each vertex of a graph is associated with a continuous-time signal [9]. This allows us to perform discrete sampling in both the graph vertex and time domain, i.e., we employ a spatio-temporal sampling. Moreover, it presents an opportunity to exploit the additional correlation information captured in the graph signals to enhance the signal recovery methods.

If the signals do not have time components, we are restricted to graph signals in the traditional sense [1]. An important special case is imaging. Pixel values can be considered as signals on a grid graph. If the pixel values of an image are folded, we obtain a *folded image* (e.g., Fig. 2). The method proposed in the paper can be used to recover folded images as we shall illustrate with a few examples in Section V.

In this paper, we consider recovery of a graph signal bandlimited to the first K eigenvectors of the graph shift operator in the vertex domain and to the baseband frequency band $[-B, B]$ Hz in the time domain. If the signal samples are *unfolded*, the Nyquist-Shannon rate for perfect signal recovery is $2BK$ Hz, i.e., recovery can be achieved by sampling at a rate of $2B$ Hz at K carefully chosen vertices of the graph [9]. Our main contributions are summarized as follows:

- (a) We provide sufficient conditions to achieve graph signal recovery from a set of *folded*



Fig. 2. Examples of grayscale folded images. The recovered images are given in Fig. 9 of Section V.

samples with sampling rate $2B(K + 1)$ Hz. In particular, we show that under a linear independence condition, only a single vertex signal in addition to the K chosen vertices for unfolded recovery needs to be sampled at a rate of $2B$ Hz. Note that the sampling rate of $2B(K + 1)$ Hz is lower than $2BK_e$ Hz if we apply the finite-order difference approach of [21] to each vertex signal individually.

- (b) To achieve practical recovery of a continuous-time graph signal from folded samples, we propose a sparse optimization procedure that is scalable. We introduce the novel concept of partition complexity for graph signals and show how to achieve minimal partition complexity through a greedy algorithm. We show that the degree of freedom in our sparse optimization, which we call λ -sparsity, is bounded by a partition complexity. This then allows us to formulate an effective sparse L^1 optimization problem.
- (c) We apply our recovery method on various continuous-time graph signals and images, including a folded image from a mouse brain [30] and images from MIT-Adobe FiveK Dataset. We provide insights on how our proposed recovery method can be adapted in practice and discuss its performance.

A preliminary version of this work was presented in [31]. In this paper, we present rigorous proofs of all results and included further experiments and tests of our approach on folded network signals and images.

The rest of the paper is organized as follows. In Section II, we present our system model and assumptions. We show that recovery of a graph signal bandlimited in both vertex and time domains can be achieved by sampling at an additional node using the Nyquist-Shannon rate in the time direction. In practice, the graph signal can be recovered by integer programming, which

becomes intractable when the size of graph grows. To mitigate this, we introduce the concept of partition complexity in Section III, which then allows us to formulate a sparse optimization based algorithm for signal recovery in Section IV. The proposed recovery method leverages on the signal correlations in both the graph and time domain for efficient signal reconstruction. We present simulation and experiment results in Section V and conclude in Section VI.

Notations. We use \mathbb{R} and \mathbb{Z} to denote the set of real numbers and integers, respectively. Suppose $x : V \mapsto \mathbb{R}$ is a mapping from a set V to \mathbb{R} . Then, for a subset $S \subset V$, we let $x(S) = (x(v))_{v \in S}$. For a matrix W , W_S is the submatrix consisting of the rows of the matrix W indexed by the set S . Thus, W_u is the row u of W .

II. FOLDED GRAPH SIGNALS

In this section, we present our system model and assumptions. We also derive a sufficient condition under which perfect recovery from folded graph signal samples is achievable. Consider an undirected, simple graph $G = (V, E)$ with V the set of vertices and E the set of edges. Let $x = (x(v, t))_{v \in V, t \in \mathbb{R}}$ be a *continuous-time graph signal*, where for each vertex $v \in V$, $x(v, \cdot) : \mathbb{R} \mapsto \mathbb{R}$ is a L^2 function [9]. Component-wise, for each $t \in \mathbb{R}$, $x(\cdot, t) = (x(v, t))_{v \in V}$ is a graph signal; and for each $v \in V$, $x(v, \cdot) = (x(v, t))_{t \in \mathbb{R}}$ is a continuous-time signal at v . Note the x is a generalized graph signal as defined by [9]. We start with the following bandlimit assumptions.

Assumption 1. *For each time t , the graph signal $x(\cdot, t)$ is spanned by $W = \{w_1, \dots, w_K\}$, K eigenvectors of the associated eigenvalues of the Laplacian matrix L of the graph G [1].*

We use W to denote the matrix with w_i as the columns. At any time t , $x(\cdot, t)$ can be represented using the basis vector coefficients $b_t = (b_{k,t}) \in \mathbb{R}^K$ as

$$x(\cdot, t) = Wb_t = \sum_{1 \leq k \leq K} b_{k,t} w_k. \quad (2)$$

As discussed in [10], [11], at each time t , we can sample the graph signal by recording the signal at a subset S of V to obtain the spatially sampled signal $x(S, t)$. The submatrix of W formed by taking the rows indexed by S is denoted by W_S . The sampled signal can be used to recover the full graph signal if the sampled nodes are chosen such that the corresponding basis matrix W_S of size $K \times K$ is invertible.

It is common to have W consisting of eigenvectors corresponding to the K smallest eigenvalues of L , for example, when one performs graph signal smoothing by using a low-pass filter.

Assumption 2. *At each node $v \in V$, the L^2 function $x(v, \cdot)$ is assumed to be bandlimited to $[-B, B]$ Hz.*

If we sample x discretely with a subset $U \subset V \times \mathbb{R}$, a useful measure is the *sampling rate* of U defined as:

$$\limsup_{a \rightarrow \infty} \frac{|(V \times [-a, a]) \cap U|}{2a}.$$

Using a sampling interval T_0 , the discrete signal

$$y = (y(v, n))_{v \in V, n \in \mathbb{Z}} = (x(v, nT_0))_{v \in V, n \in \mathbb{Z}}$$

is obtained. Applying the Nyquist-Shannon sampling rate, we may choose $T_0 = 1/(2B)$ for complete signal recovery of $x(v, \cdot)$ from the sampled discrete signal y . Using both spatial and temporal sampling, a sampling rate of $2BK$ over the entire graph guarantees a perfect recovery of the full signal. The concept of a \mathcal{F} -transform for generalized graph signals was developed in [9] to quantify the variation of the signal using the joint spectrum over the graph vertex and time domains. The \mathcal{F} -transform of x in (2) evaluated at the k -th graph eigenvalue and time domain frequency f , where $k \in \{1, \dots, K\}$ and $f \in [-B, B]$, is given by

$$d_{k,f} = \frac{1}{2\pi} \int_{\mathbb{R}} b_{k,t} e^{-i2\pi t f} dt,$$

which is also the Fourier transform of $b_{k,t}$ if we consider it to be a continuous-time signal.

Assumption 3. *For each $k = 1, \dots, K$ and $f \in [-B, B]$,*

$$|d_{k,f}| \leq a_{k,f}. \quad (3)$$

Assumption 3 is used in the quantitative analysis in Section III-B.

We consider the scenario where the graph signal is not recorded perfectly by the ADC, e.g., the signal dynamic range exceeds the voltage range of the ADC. We use self-reset ADCs to sample the graph signal. A self-reset ADC captures the signal at each sampled node and yields a folded signal via a modulo operation. More specifically, the maximum amplitude that can be measured by the ADC, a positive real number λ , is called the *folding rate*. Using the definition

of a modulo operator described in (1), the graph signal $y(S, n) = (y(v, n))_{v \in S} \in \mathbb{R}^K$ can be expressed as follows:

$$y(S, n) = D_\lambda z(S, n) + p(S, n), \quad (4)$$

where D_λ is a diagonal matrix with diagonal entries all equal to λ and $0 \leq p(v, n) < \lambda$ for all $v \in S$. We refer to $z(S, n) \in \mathbb{Z}^K$ as the vector of folding numbers and $p(S, n) \in [0, \lambda)^K$ as the vector of folded signals.

For an invertible matrix W_S , the basis coefficients b_{i,nT_0} , and hence $y(\cdot, n)$, are uniquely determined by $y(S, n)$. However, if we only observe $p(S, n)$, it is in general not enough to recover $y(\cdot, n)$, and additional information is required.

To state such information, we need one more notion: k real numbers a_1, \dots, a_k are said to be *linearly independent over \mathbb{Z}* if the only integer solution to the equation $\sum_{1 \leq i \leq k} a_i x_i = 0$ is $x_i = 0$ for all $1 \leq i \leq k$. It is common to have k -tuples linearly independent over \mathbb{Z} by countability.

Theorem 1. *Consider graph signals that belong to the span of $W = \{w_1, \dots, w_K\}$. Let $S \subset V$ be a subset of sampled nodes of size K such that the submatrix W_S formed by taking the rows of W indexed by S is invertible. Suppose that folded signals with folding rate λ are observed at vertices in S . We have the following:*

- (a) *Let $u \in V \setminus S$ be an additional node such that the entries of $W_u W_S^{-1}$ are linearly independent over \mathbb{Z} . If the folding rate λ' at u is chosen according to a probability distribution absolutely continuous with respect to (w.r.t.) the Lebesgue measure, then with probability one, any graph signal $x : V \mapsto \mathbb{R}$ can be recovered from the folded signals of x at $V' = S \cup \{u\}$.*
- (b) *If $u \in V \setminus S$ with folding rate λ such that $W_u W_S^{-1}$ contains an irrational entry, then there are infinitely many x with the same folded signals at S and distinct folded signals at u .*

Proof:

- (a) Consider two graph signals $x = \sum_{1 \leq i \leq K} a_i w_i$ and $\hat{x} = \sum_{1 \leq i \leq K} \hat{a}_i w_i$, with the corresponding vectors of folded signals and folding numbers at the sample set S given by $\{p, z\}$ and $\{\hat{p}, \hat{z}\}$, respectively. Suppose $p = \hat{p}$. We want to show that if x and \hat{x} have the same folded sample at u with folding rate λ' randomly chosen according to a distribution absolutely continuous w.r.t. the Lebesgue measure, then with probability one, $z = \hat{z}$ and hence $x = \hat{x}$.

Since $p = \hat{p}$, we have

$$\sum_{1 \leq i \leq K} (\hat{a}_i - a_i) w_i = D_\lambda q, \quad (5)$$

where $q = \hat{z} - z \in \mathbb{Z}^K$ is the difference in the folding numbers of the two graph signals \hat{x} and x at the sample set S . For a node $u \notin S$, write $W_u = (w_i(u))_{1 \leq i \leq K}$. The following holds:

$$\hat{x}(u) - x(u) = \sum_{1 \leq i \leq K} (\hat{a}_i - a_i) w_i(u). \quad (6)$$

Combining (5) together with (6), and since W_S is invertible, we have

$$\begin{aligned} \hat{x}(u) - x(u) &= \lambda W_u W_S^{-1} q, \\ &= \lambda \sum_{1 \leq j \leq K} q_j (W_u W_S^{-1})_j, \end{aligned} \quad (7)$$

where q_j and $(W_u W_S^{-1})_j$ are the j -th components of the vectors q and $W_u W_S^{-1}$, respectively. If $q_j, 1 \leq j \leq K$ are not all 0, then as the entries of $W_u W_S^{-1}$ are linearly independent over \mathbb{Z} , the expression $\lambda \sum_{1 \leq j \leq K} q_j (W_u W_S^{-1})_j$ is non-zero. Moreover, if q varies over $\mathbb{Z}^K \setminus \{0\}$, the collection $\Delta = \left\{ \lambda \sum_{1 \leq j \leq K} q_j (W_u W_S^{-1})_j : q \in \mathbb{Z}^K \setminus \{0\} \right\}$ is a countable set in \mathbb{R} . We have seen that $0 \notin \Delta$. Hence, the set $\Lambda = \{\lambda' : \delta/\lambda' \in \mathbb{Z} \text{ for some } \delta \in \Delta\}$ is countable and has Lebesgue measure zero. Therefore, with probability one, a randomly chosen λ' does not belong to Λ . Consequently, with such λ' , if x and \hat{x} has the same folded sample at u , then $q = 0$.

- (b) Without loss of generality, we assume that $r = (W_u W_S^{-1})_1$ is irrational. In (7), we let $q_j = 0$ for $j > 1$ and let q_1 vary over \mathbb{Z} . With such a choice, as r is irrational, the folded values of $\hat{x}(u) - x(u) = \lambda q_1 r$ are dense in the interval $[0, \lambda)$. In particular, there are infinitely many possibilities for $\hat{p}_u - p_u$. Therefore, we can observe the same folded signals at S and different folded signals at u for infinitely many x . ■

One should note that Theorem 1(a) does not rule out the possibility $\lambda' = \lambda$. From the proof, we can choose $\lambda' = \lambda$ if $\sum_{1 \leq j \leq K} q_j (W_S^{-1} W_u^T)_j$ is irrational for some $(q_j)_{1 \leq j \leq K} \in \mathbb{Z}^K$. In Appendix A, we demonstrate that the conditions in Theorem 1 as well as the above condition for $\lambda' = \lambda$ are satisfied generally in certain random models.

In practice, say a sensor network, the random folding rate at an additional node required in Theorem 1(a) can be realized by setting one of the sensor nodes to operate at a lower folding

rate λ' than its maximum voltage level λ , choosing it uniformly randomly in $(0, \lambda)$. We would like to point out that λ' appearing in the theorem is independent of the signal x . Therefore, as long as G and W are fixed and the conditions of Theorem 1(a) are satisfied, we are able to recover the graph signal from folded samples. This leads to the following.

Corollary 1 (Discrete sampling rate). *Suppose W, S, u and λ' are the same as in Theorem 1(a). There are discrete subsets $S_1, S_2 \subset V \times \mathbb{R}$ with sampling rate $2BK$ and $2B$ respectively such that the following holds: Consider any x such that $x(\cdot, t)$ belongs to the span of columns of W and $x(v, \cdot)$ is bandlimited by B for any $t \in \mathbb{R}, v \in V$. The generalized graph signal x can be recovered from the folded signals at S_1 with folding rate λ together with folded samples at S_2 with folding rate λ' .*

Proof: Let T' be a discrete subset of \mathbb{R} sampled at the Nyquist-Shannon rate, i.e., with sampling rate $2B$. Take $S_1 = S \times T'$ and $S_2 = \{u\} \times T'$. For each $t \in S'$, we are able to recover the entire graph signal $x(\cdot, t)$ from the folded samples at $(S \cup \{u\}) \times \{t\}$ by Theorem 1(a). Consequently, by the Nyquist-Shannon sampling theorem, we can recover $x(v, \cdot)$ for each $v \in V$ and hence the entire signal x . ■

Suppose we have a sample set S of size K with folding rate λ and another sample set S' of size $K' \geq 1$ with folding rate λ' such that W_S is invertible. In addition, we assume that for some $u \in S'$, the entries of $W_u W_S^{-1}$ are linearly independent over \mathbb{Z} . From Theorem 1(a), the folded signals at $S \cup S'$ allow us to recover the generalized graph signal. Specifically, at time nT , let the folded signals and folding numbers at S and S' be given by pairs of vectors $\{p(S, n), z(S, n)\}$ and $\{p(S', n), z(S', n)\}$, respectively. Using (4) and noting that $y(S', n) = W_{S'} W_S^{-1} y(S, n)$, we have

$$W_{S'} W_S^{-1} p(S, n) - p(S', n) = -W_{S'} W_S^{-1} D_\lambda z(S, n) + D_{\lambda'} z(S', n). \quad (8)$$

Recoverability of the signal x is equivalent to (8) having a unique integer solution. We can thus apply integer programming to recover $z(S, n)$ and $z(S', n)$. This makes our approach local in nature. This means that in each stage of the recovery scheme, we only need to consider finitely many sampled nodes, concentrated in a short time interval. It can also be applied to snapshot graph signal recovery from observations of folded signals at appropriately chosen sample nodes. Moreover, it can also locally recover signals that fail to fulfill global bandlimited or L^2 assumptions in the time direction.

Regarding sampling rate, a direct application of the unlimited sampling algorithm proposed in [21] for the signal at each vertex of the graph yields an overall sampling rate of $2BK_e$. In our proposed approach, by optimally exploiting the graph correlation information, a sampling rate of $2B(K+1)$ over the entire graph is achievable by choosing $K' = 1$. This rate is significantly smaller than $2BK_e$ for large K and B . However, integer programming is intractable for large K . In the following, we propose an alternative sparse recovery method that is however suboptimal. We utilize both the spatial and temporal correlations to recover the signal. The main idea is to choose a sample set of vertices $V' = S \cup S'$ so that it can be further partitioned into subsets on which the graph signal do not vary much at each time instant. Each of these subsets of vertices then share “approximately” the same folding number at each time instant. In the following section, we introduce the concept of *partition complexity* and show how it is related to the degrees of freedom in the graph signal.

III. GRAPH SAMPLING

Recall that *sampling* on $G = (V, E)$ refers to selecting a subset of nodes $V' \subset V$, so that certain requirements are met. The signal recovery problem from folded signals is equivalent to the recovery of the folding numbers. In this paper, we want to sample nodes whose signals tend to have small differences. This is because, at such nodes, the folding numbers have greater chance to be similar.

A. Partition complexity

We need a way to quantify the difference between the signals at two different vertices. To do this, we utilize a symmetric non-negative “distance” function that will be carefully designed in the next Section III-B to account for the graph signal’s bandlimitedness in both the graph vertex and time domains. We then wish to partition a set of sampled vertices into subsets of vertices that are close to each other in terms of this “distance” function. We start with a basic definition. See Fig. 3 for a simple illustration.

Definition 1. Suppose $\phi : V \times V \rightarrow \mathbb{R}_{\geq 0}$ is a symmetric non-negative function on pairs of vertices of G . Let $r > 0$ be a real number and $V' \subset V$ be a subset of nodes. A (ϕ, r) -admissible partition of V' is a decomposition of V' into a union of subsets $V' = \bigcup_{1 \leq i \leq k} V_i$ such that for each component V_i , there is a center $v_i \in V_i$ and $\phi(v_i, v) < r$ for all $v \in V_i$. The smallest k

such that V' has an admissible partition into k -components is called the (ϕ, r) -complexity of V' , denoted by $c_{\phi, r}(V')$.

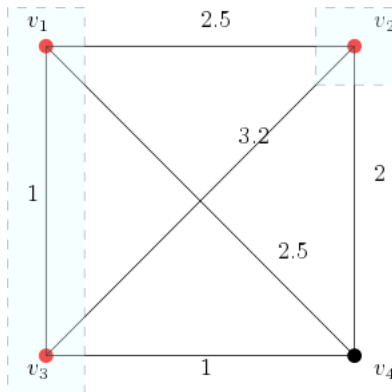


Fig. 3. Let $V = \{v_1, v_2, v_3, v_4\}$ with 4 nodes and $V' = \{v_1, v_2, v_3\}$. The values of the function ϕ are labeled along the edges. If $r = 2$, the complexity $c_{\phi, r}(V') = 2$. In this case, we apply the partition $V' = \{v_1, v_3\} \cup \{v_2\}$ with centers v_1 and v_2 respectively. On the other hand, if $r = 3$, then $c_{\phi, r}(V') = 1$. The partition $V' = V'$ is trivial, and the center must be chosen as v_1 . Moreover, in the case $r = 2$, we have $\min_{|V'| \geq 3} c_{\phi, r}(V') = 1$. We can choose $V' = \{v_1, v_3, v_4\}$ with center v_3 .

For fixed ϕ and r , as we will see in Section III-B, it is desirable to find a subset of nodes V' with size bounded below by an integer $s \leq |V|$ such that the (ϕ, r) -complexity of V' is as small as possible. This is re-cast as the following optimization problem:

$$\min_{|V'| \geq s} c_{\phi, r}(V'). \quad (9)$$

To solve Problem (9), we can consider it from a different angle. For each $v \in V$, the ϕ -ball of radius r at v is defined as the set $B_{\phi, r}(v) = \{v' \in V : \phi(v, v') < r\}$. For each (ϕ, r) -admissible partition $V' = \cup_{1 \leq i \leq k} V_i$, we have $V_i \subset B_{\phi, r}(v_i)$, where v_i is a center. Therefore, Problem (9) is equivalent to the following optimization problem:

$$\min_{\substack{|\cup_{1 \leq i \leq k} B_{\phi, r}(v_i)| \geq s, \\ v_1, \dots, v_k \in V}} k. \quad (10)$$

Definition 2. For a fixed integer $0 < k \leq |V|$ and a subset S of V of size k , we use $B_{\phi, r}(S)$ to denote the union $\cup_{s \in S} B_{\phi, r}(s)$, and call this the ϕ -ball centered around S .

To solve Problem (10), we may estimate $\max_{|S|=k} |B_{\phi, r}(S)|$, starting from $k = 1$. Regarding the size of $B_{\phi, r}(S)$, we have the following observation.

Lemma 1. The function $S \mapsto |B_{\phi, r}(S)|, S \subset V$ is a submodular set function.

Recall that there are several equivalent characterizations for submodularity and we describe one such characterization here. Let Ω be a set. A function $F : 2^\Omega \rightarrow \mathbb{R}$ on subsets of Ω is *submodular* if and only if the following holds: for any $X \subset Y \subset \Omega$ and $x \in \Omega \setminus Y$, we have:

$$F(X \cup \{x\}) - F(X) \geq F(Y \cup \{x\}) - F(Y). \quad (11)$$

We now proceed to the proof of Lemma 1 with (11) as the definition of submodularity.

Proof: Given $S_1 \subset S_2 \subset V$ and $v \in V$, we have the obvious inclusion

$$B_{\phi,r}(v) \setminus B_{\phi,r}(S_2) \subset B_{\phi,r}(v) \setminus B_{\phi,r}(S_1).$$

Therefore, the function $S \mapsto |B_{\phi,r}(S)|$ is submodular following the above definition. \blacksquare

Maximizing a submodular function with size constraint is usually intractable. However, the *greedy algorithm* gives a reasonable approximation [32]. Therefore, we propose the following algorithm for Problem (10): we initialize by choosing $S = \{v\}$ such that $|B_{\phi,r}(v)|$ is maximized. In each subsequent iteration, we add a new node v to S such that $|B_{\phi,r}(S \cup \{v\})|$ is maximized. The procedure terminates when $|B_{\phi,r}(S)| \geq s$.

B. λ -sparsity

We start with the following notion of λ -sparsity, which quantifies the degrees of freedom the folding numbers of a signal can have.

Definition 3. Given a vector $x = (x_i)_{1 \leq i \leq n}$ written as $x = D_\lambda z + p$ with $z \in \mathbb{Z}^n$ and $0 \leq p_i < \lambda, 1 \leq i \leq n$, the λ -sparsity of x is defined as the smallest size of a subset $I \subset \{1, \dots, n\}$ such that $z = (z_1, \dots, z_n)$ is uniquely determined by $\{z_i : i \in I\}$.

Intuitively, given a signal x , we would like to use λ -sparsity to count the amount of “different” folding numbers when x is folded w.r.t. λ . We now apply the results in Section III-A by introducing an explicit non-negative symmetric function $\phi : V \times V \rightarrow \mathbb{R}_{\geq 0}$ as follows:

$$\phi(u, v) = \sqrt{2} \sum_{1 \leq i \leq K} \int_{-B}^B a_{i,f} \sqrt{1 - \cos \frac{\pi f}{B}} df \cdot |w_i(u) - w_i(v)|, \quad (12)$$

with B as in Assumption 2, and $a_{i,f}$ as in Assumption 3.

Consider a bandlimited continuous-time graph signal x . Suppose we choose a discrete subset of samples $V' \times T$ in $V \times \mathbb{R}$, where $T = \{t_i : i \in \mathbb{Z}\}$ are time instances uniformly spaced by $1/(2B)$, i.e., at the Nyquist-Shannon rate. Let $x(V', \cdot)$ be the restriction of the signal x to V' . To

elucidate the reason behind our choice of ϕ , we have the following estimate on the λ -sparsity regarding $x(V', \cdot)$.

Theorem 2. *For any $i \in \mathbb{Z}$, the λ -sparsity of the difference $x(V', t_i) - x(V', t_{i+1})$ is upper bounded by the $(\phi, \lambda/2)$ -complexity $c_{\phi, \lambda/2}(V')$ of V' .*

Proof: We first remark that given $y_1 = \lambda z_1 + p_1$ where p_1 is the folded signal of y_1 , and given the folded signal p_2 of $y_2 = \lambda z_2 + p_2 \in (y_1 - \lambda/2, y_1 + \lambda/2)$, then the folding number z_2 of y_2 is uniquely determined (see Fig. 4): if $p_2 - p_1 \geq \lambda/2$, then the $z_2 = z_1 - 1$. If $p_1 - p_2 \geq \lambda/2$, then $z_2 = z_1 + 1$. Otherwise, $z_2 = z_1$.

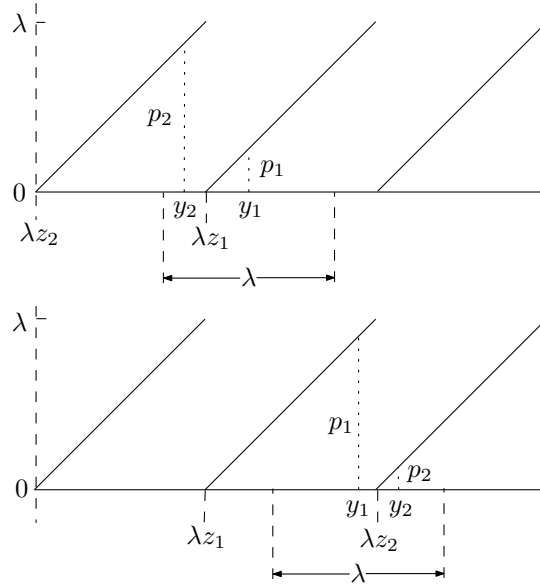


Fig. 4. The modulo operation is injective over an interval of length λ . Therefore, if $|y_2 - y_1| < \lambda/2$, then the folding number of y_2 is uniquely determined by the folding number of y_1 .

With Assumption 2, we can express the continuous-time graph signal x as

$$x(v, t) = \sum_{i=1}^K \int_{-B}^B d_{i,f} e^{i2\pi t f} df \cdot w_i(v),$$

for a family of coefficients $d_{i,f}$, $1 \leq i \leq K$, $f \in [-B, B]$ such that $|d_{i,f}| \leq a_{i,f}$.

If $t_{i+1} - t_i = 1/(2B)$ and $u, v \in V'$, then

$$\begin{aligned} & |(x(u, t_i) - x(u, t_{i+1})) - (x(v, t_i) - x(v, t_{i+1}))| \\ &= \left| \sum_{i=1}^K \int_{-B}^B d_{i,f} (e^{2\pi i t_{i+1} f} - e^{2\pi i t_i f}) df \cdot (w_i(u) - w_i(v)) \right| \end{aligned}$$

$$\begin{aligned}
&\leq \sum_{i=1}^K \int_{-B}^B a_{i,f} \cdot \sqrt{2} \sqrt{1 - \cos\left(\frac{\pi f}{B}\right)} df \cdot |w_i(u) - w_i(v)| \\
&= \phi(u, v),
\end{aligned} \tag{13}$$

where the inequality follows from the assumption that $|d_{i,f}| \leq a_{i,f}$ and the equality

$$|e^{i2\pi(t+1/(2B))f} - e^{i2\pi tf}| = \sqrt{2 \left(1 - \cos \frac{\pi f}{B}\right)}, \text{ for } t \in \mathbb{R}.$$

For convenience, let $y = x(V', t_i) - x(V', t_{i+1})$. Suppose

$$V' = \bigcup_{1 \leq i \leq c_{\phi, \lambda/2}(V')} V_i$$

is an admissible partition with centers $v_i \in V_i$. Then for each $v \in V_i$, we have $\phi(v_i, v) < \lambda/2$ and from (13), $|y(v_i) - y(v)| < \lambda/2$. As a consequence, the folding number of $y(v)$ is determined by the folding number of $y(v_i)$. Consequently, the λ -sparsity of y is at most $c_{\phi, \lambda/2}(V')$. ■

In applications, we may relax $\lambda/2$ by allowing a perturbation $\lambda/2 + \epsilon$ with some suitable choice of $\epsilon > 0$. The consequence is that we may have a smaller partition complexity, at the cost of losing $c_{\phi, \lambda/2+\epsilon}$ being the theoretical upper bound of λ -sparsity. This can be useful if the $a_{i,f}$'s in ϕ are not tight. We explore the effect of adding ϵ in Section V.

IV. GRAPH SIGNAL RECONSTRUCTION

In this section, we make use of the concepts introduced in the previous section to develop an algorithm that recovers a generalized graph signal using the folded samples recorded by self-reset ADCs. This is equivalent to recovering the folding numbers.

Suppose we have samples S of size K with folding rate λ and S' of size K' with folding rate λ' such that W_S is invertible. In addition, we assume that for some $u \in S'$, the entries of $W_u W_S^{-1}$ are linearly independent over \mathbb{Z} . From Theorem 1, these properties guarantee theoretical perfect recovery. See also Appendix A for sufficient conditions under which these properties hold. At each time nT , where $T = 1/(2B)$ and $n \in \mathbb{Z}$, let the folded signals and folding numbers at S and S' be given by pairs of vectors $\{p(S, n), z(S, n)\}$ and $\{p(S', n), z(S', n)\}$, respectively.

Lemma 2. *If the continuous-time graph signal x is in $L^2(V \times \mathbb{R})$, then $z = (z(v, t))_{v \in V, t \in \mathbb{R}}$ where $z(v, t)$ is the folding number of $x(v, t)$, is compactly supported.*

Proof: As V is finite, it suffices to show that $z(v, \cdot)$ is compactly supported for each $v \in V$. As $x \in L^2(V \times \mathbb{R})$, $x(v, \cdot)$ belongs to $L^2(\mathbb{R})$. By Assumption 2 and the Whittaker-Shannon interpolation formula [33],

$$x(v, t) = \sum_{n \in \mathbb{Z}} x(v, nT) \operatorname{sinc}\left(\frac{t}{T} - n\right),$$

for $T = 1/(2B)$. As integer translates of the sinc function are pairwise orthogonal with the same L^2 -norm, the sum $\sum_{n \in \mathbb{Z}} |x(v, nT)|^2$ is finite. In particular, $|x(v, nT)| \rightarrow 0$ as $|n| \rightarrow \infty$ and $|x(v, nT)|$ is bounded, say by b . For $N_0 \in \mathbb{Z}$, we have

$$\begin{aligned} |x(v, t)| &= \left| \sum_{n \in \mathbb{Z}} x(v, nT) \operatorname{sinc}(t/T - n) \right| \\ &\leq \sum_{n < N_0} |x(v, nT)| \cdot |\operatorname{sinc}(t/T - n)| + \sum_{n \geq N_0} |x(v, nT)| \cdot |\operatorname{sinc}(t/T - n)| \\ &\leq b \sum_{n < N_0} |\operatorname{sinc}(t/T - n)| + \sup_{n \geq N_0} \{|x(v, nT)|\} \sum_{n \in \mathbb{Z}} |\operatorname{sinc}(t/T - n)|. \end{aligned}$$

We can always choose N_0 such that $\sup_{n \geq N_0} \{|x(v, nT)|\}$ is arbitrarily small. At the same time, for any $|t|$ large enough, $\sum_{n < N_0} |\operatorname{sinc}(t/T - n)|$ can be made arbitrarily small. Therefore, $|x(v, t)| \rightarrow 0$ as $|t| \rightarrow \infty$. Thus, as $|t| \rightarrow \infty$, $x(v, t)$ does not fold, and z must be compactly supported. \blacksquare

Recall from (4) that $y(\cdot, n)$, $n \in \mathbb{Z}$, are samples of x at discrete time instances. For square integrable bandlimited x , by Lemma 2, the discrete samples $y(\cdot, n)$ are unfolded for large $|n|$. Hence, it suffices to recover the folding number for each $y(\cdot, n+1) - y(\cdot, n)$. In the case of clipping, i.e., we do not observe $y(\cdot, n)$ when $|n|$ is large, our method recovers the folding numbers up to an additive constant as in [21].

Fix an n and let $\bar{y}(\cdot) = y(\cdot, n+1) - y(\cdot, n)$. Denote the folding numbers and folded signals of $\bar{y}(\cdot)$ by $\bar{z}(\cdot)$ and $\bar{p}(\cdot)$, i.e., $\bar{y}(\cdot) = D_\lambda \bar{z}(\cdot) + \bar{p}(\cdot)$. From (8), we obtain

$$W_{S'} W_S^{-1} \bar{p}(S) - \bar{p}(S') = D_\lambda \bar{z}(S') - W_{S'} W_S^{-1} D_\lambda \bar{z}(S). \quad (14)$$

Our signal recover steps are as follows:

Step 1: For a fixed $K' \geq 1$, we proceed by using the greedy algorithm to solve Problem (10) in Section III-A to obtain a sample set of vertices V' of size $K + K'$ such that V' has (approximately) minimal $(\phi, \lambda/2)$ -complexity. Decompose $V' = S \cup S'$ such that $|S| = K$ and W_S is invertible. Write $V' = \cup_{1 \leq i \leq c} V_i$ as a disjoint partition where V_i has center c_i .

Step 2: We replace the unknowns $\{\bar{z}(S), \bar{z}(S')\}$ in (14) by variables $\zeta = (\zeta(v))_{v \in V'}$ as follows (cf. proof of Theorem 2):

- (a) If $v = c_i$ for some $i = 1, \dots, c$, make the substitution $\bar{z}(c_i) = \zeta(c_i)$.
- (b) Suppose that $v \in V_i$. If $\bar{p}(v) - \bar{p}(c_i) \geq \lambda/2$, write $\bar{z}(v) = \zeta(c_i) + \zeta(v) - 1$. If $\bar{p}(c_i) - \bar{p}(v) \geq \lambda/2$, write $\bar{z}(v) = \zeta(c_i) + \zeta(v) + 1$. For the remaining cases, write $\bar{z}(v) = \zeta(c_i) + \zeta(v)$.

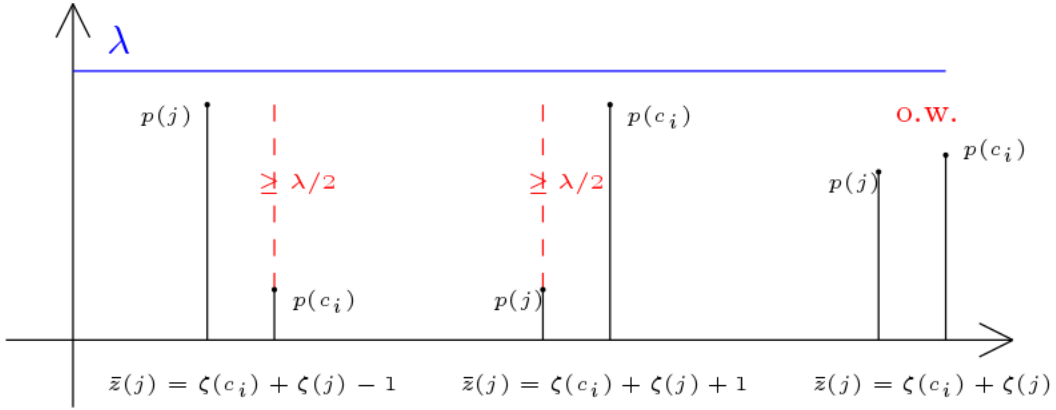


Fig. 5. Illustration of the substitution of \bar{z} by ζ in Step 2.

The above substitution is illustrated by Fig. 5. In (b), if $v \in V_i$ and the signal at vertices c_i and v differ less than $\lambda/2$, then $\zeta(v) = 0$. Hence, if the above holds for most such pairs c_i and v , we have a sparse solution in the variables $\zeta(v)$.

Step 3: We obtain a new set of equations on the $K + K'$ variables $\zeta = (\zeta(v))_{v \in V'}$ expressed as

$$M\zeta = g \quad (15)$$

with M being a $(K + K') \times K'$ matrix. As we observed earlier, $\zeta(v) = 0$ unless $v = c_i$ for some center. In this case, ζ in (15) can be solved exactly if $\text{rank}(M) \geq c_{\phi, \lambda/2}(V')$ by Theorem 2. However, if the bound $a_{i,f}$ in Assumption 3 is not tight, neither is the bound by the function ϕ in (13). In this case, the $(\phi, \lambda/2)$ -complexity of any $V' \subset V$ might be large. We may instead sample V' with small $(\phi, \lambda/2 + \epsilon)$ -complexity for $\epsilon > 0$. We no longer expect (15) can be solved directly. However, at the compensation of a smaller partition complexity $c_{\phi, \lambda/2 + \epsilon}(V')$, we expect ζ is sparse. Therefore, we heuristically propose solving:

$$\begin{aligned} \min \quad & \|\zeta\|_1, \\ \text{s. t.} \quad & M\zeta = g. \end{aligned} \quad (16)$$

Moreover, suppose that at vertex v the folding number $\bar{z}(v)$ is observed and v belongs to V_i . This gives us an additional equation taking one of the forms: $\bar{z}(v) = \zeta(c_i) + \zeta(v) - 1$, $\bar{z}(v) = \zeta(c_i) + \zeta(v) + 1$ or $\bar{z}(v) = \zeta(c_i) + \zeta(v)$, which can be added to the linear constraints of Problem (16).

V. SIMULATION AND EXPERIMENT RESULTS

In this section, we present simulation results to demonstrate the performance of our method on folded continuous-time graph signals. We then conduct experiments on folded images to validate that our approach can recover the original unfolded image. To the best of our knowledge, our work is the first to consider the recovery of folded graph signals. Therefore, there are no existing benchmarks that we can compare with.

A. Folded continuous-time graph signals

We consider G being one of the following graphs: the complete graph with discrete random edge weights, the Arizona power plant network [34] as illustrated in Fig. 6, and 2-dimensional (2D) lattice of size 25×20 . A power plant may observe signals with high dynamic range such as temperature measurements [35]. On the other hand, a lattice can be used to model an image carrying HDR pixel values. For the parameters in Assumptions 1-3, we standardize the bandlimit B to be 1 Hz and set $a_{i,f}$ to be inversely proportional to i and f . The choice of K and K' are summarized in Table I.

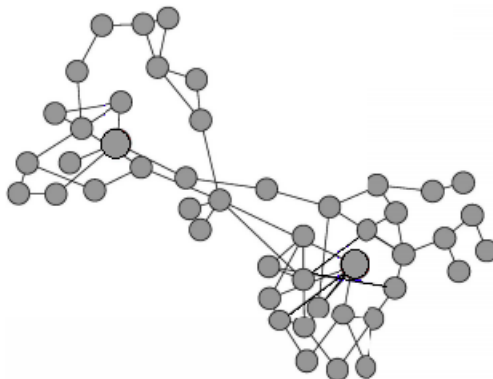


Fig. 6. A part of the Arizona power plant network (modified from Fig. 8 of [36]).

TABLE I
 K AND K' FOR DIFFERENT GRAPHS.

Graph	size	K	K'
Complete graph	120	50	20
Power plant	47	20	10
2D lattice	500	80	30

For each simulation instance, each coefficient of the signal x w.r.t. the basis is chosen uniform randomly within the bounded set by the corresponding $a_{i,f}$. The folding rate λ is chosen to ensure significant amount of non-zero foldings. In addition, we add white Gaussian noise to the observed folded signals with the signal-to-noise ratios (SNR) being 15 dB, 20 dB, and 40 dB. As discussed in Section IV, we aim at recovering the difference signals. An example of a continuous-time graph signal and its folded version is shown in Fig. 8.

Due to noise, we apply the proposed recovery algorithm by solving the following modified version of Problem (16) to recover the difference signal:

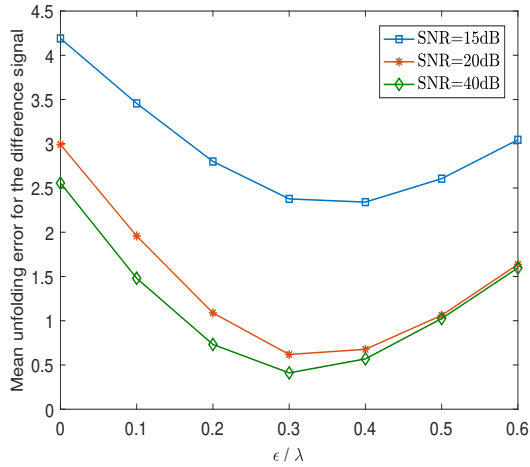
$$\min \|\zeta\|_1 + \alpha \|M\zeta - g\|_2^2, \quad (17)$$

where α is a chosen regularizing parameter.

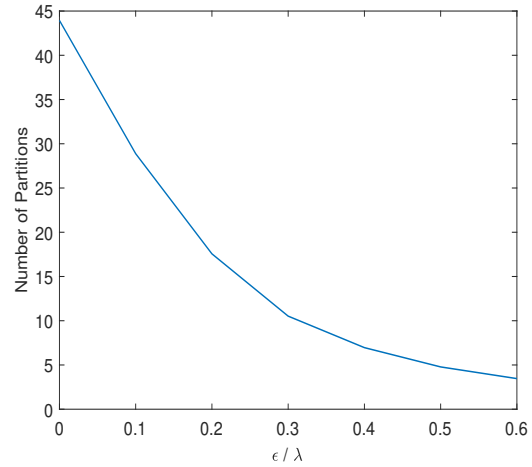
We choose the set of sample nodes V' with small $(\phi, \lambda/2 + \epsilon)$ -complexity by the greedy algorithm. For different values of ϵ , we plot in Fig. 7 the average total recovery error in the folding numbers and the size of $(\phi, \lambda/2 + \epsilon)$ admissible partition of V' against ϵ/λ . Different curves correspond to different noise levels.

From the plots, we first notice that the performance gets better with less noise as expected. The errors are small if SNR = 20 dB, 40 dB. Most importantly, we see that generally as ϵ increases, the average recovery error first drops and then increases. The error is small at the minimum. The best performance occurs for ϵ when the size of $(\phi, \lambda/2 + \epsilon)$ admissible partition of V' is relatively small. In such a case, we have a balance between the partition size and amount of nodes in each partition. In addition, the best range of ϵ is independent of the noise level.

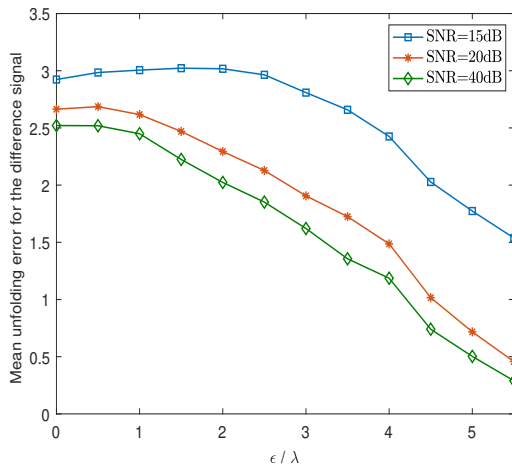
The observation made above gives us a general guideline on how to choose ϵ . One may first choose $\epsilon_1 < \epsilon_2$ such that: at ϵ_1 , the number of partitions is $\approx K + K'$; while at ϵ_2 , the number of partitions is ≈ 1 . Then one may perform a binary search scheme within the interval $[\epsilon_1, \epsilon_2]$ to identify a range of ϵ so that the partition size is appropriate.



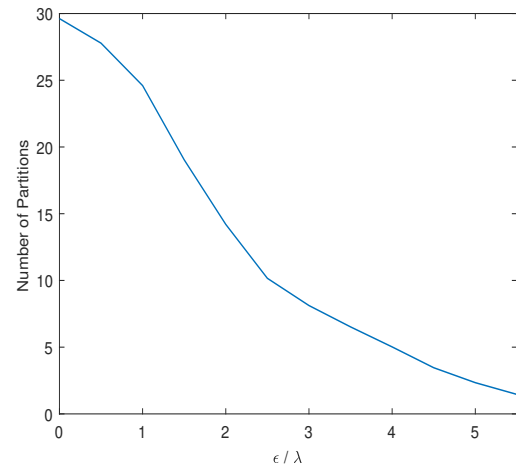
(a) Complete graph



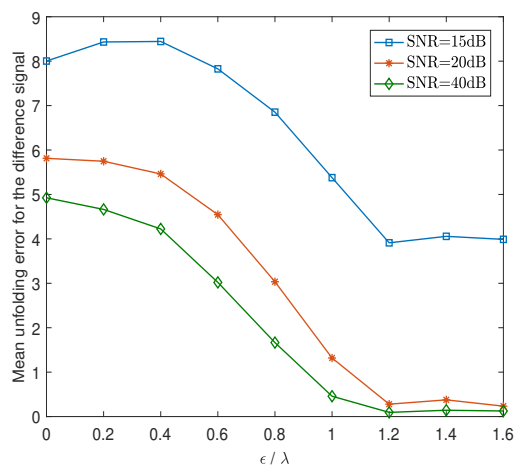
(b) Complete graph



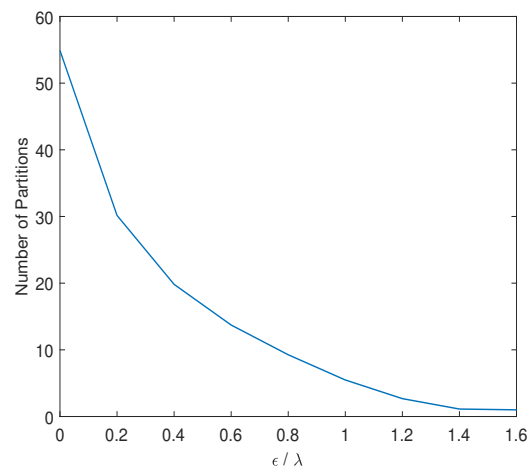
(c) Power plant



(d) Power plant



(e) 2D lattice



(f) 2D lattice

Fig. 7. The average total recovery error in folding numbers of the difference signals and the size of $(\phi, \lambda/2 + \epsilon)$ admissible partition of V' against ϵ/λ .

For illustration, we show in Fig. 8 examples of the recovery of continuous-time folded graph signals. Fig. 8(a) shows an example with relatively good recovery while Fig. 8(b) shows one with less perfect recovery. However, even in Fig. 8(b), the error in relative difference between adjacent time slots in the recovered signals is still small as compared with the relative difference of the original signal.

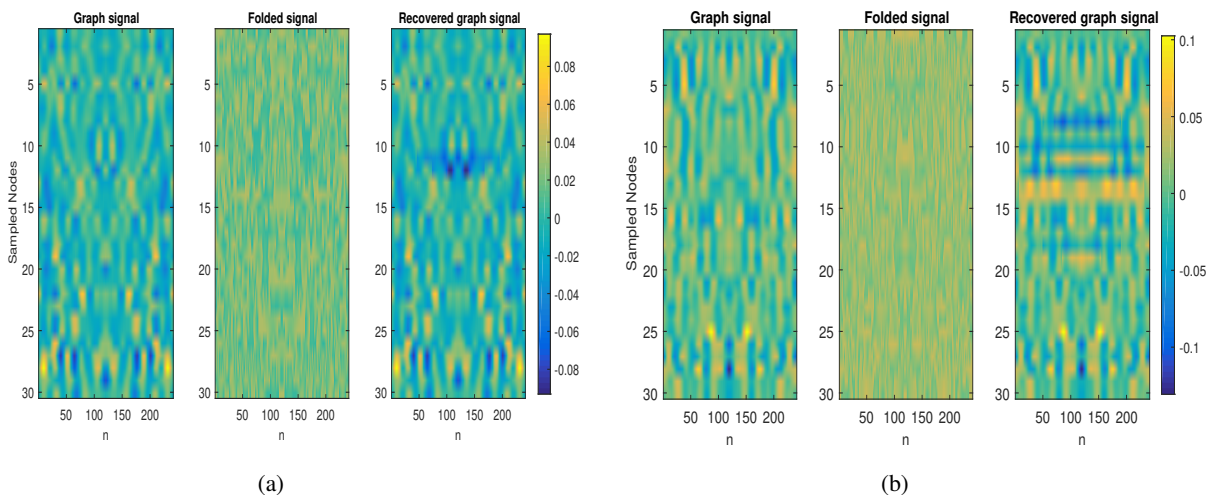


Fig. 8. The example heat maps of continuous-time folded graph signals: the original unfolded signals (left), and folded signals (middle) and the recovered signals (right). The horizontal axis is the time domain, while the vertical axis corresponds to the graph vertex domain.

B. Folded images

In this subsection, we present simulation results for folded image recovery. As there are no time component, we remove the integral factor in (12) when performing folded image recovery. For each image, let P be the total number of pixels. We express parameters such as K , K' as a factor of P for convenience.

For the toy examples in Fig. 2, the pixel values are scaled within $[0, 1]$ and the folding rate is taken to be 0.75. Fig. 2(a) has $K = 0.2P$, $K' = 0.05P$. Fig. 2(b) has $K = 0.3P$, $K' = 0.05P$. Fig. 2 looks darkened and noisy as we assign 0 at unobserved pixels, though they are not used in the recovery procedure. Using our approach described in Section IV, the images are recovered perfectly as shown in Fig. 9.

Next, we consider the recovery of a mouse brain image using a self-reset CMOS sensor [30]. In this experiment, an image sensor was created by [30] and surgically implanted onto the brain

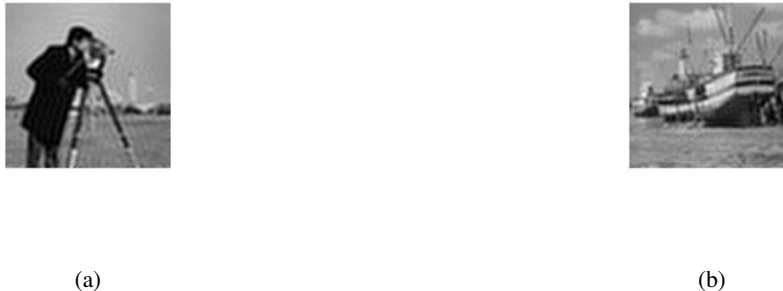


Fig. 9. Recovered images of the folded images in Fig. 2.

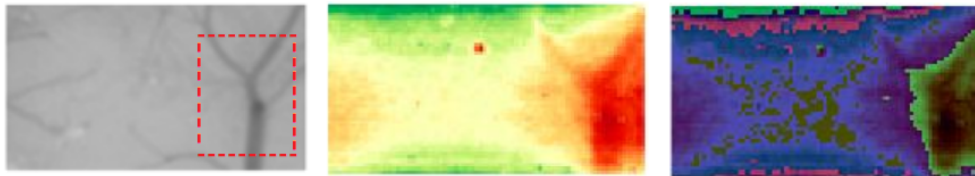


Fig. 10. The mouse brain surface images. Left: the original grayscale image with highlighted key feature. Middle: the colored image. Right: the folded image of the colored version

surface of a mouse (see Fig. 4 of [30]). The image sensor is designed with a self-reset circuit to enable it to work with high dynamic range of light intensity and SNR. The reset count of each pixel was recorded so that the original pixel light intensity value can be recovered. We make use of the folded image created by [21], which is based on the grayscale image in Fig. 7 of [30] to recover the original image. Our goal is to show that we can recover the original image without keeping track of the reset counts.

The mouse brain surface shown on the left of Fig. 10 is obtained using a microscope with white light and is provided by [30]. The key feature captured by the image is the blood vessel highlighted within the dotted square. The colored version (middle image of Fig. 10) is taken from [21] with bandlimit $K \approx 0.57P$. The blood vessel in the grayscale image is captured in the red region towards the right end. If the folding rate $\lambda = 0.7$, we obtain the folded image (right of Fig. 10). A large part of the image has non-zero folding numbers: 89%, 83%, 8% for the red, green and blue channels respectively. In the folded image, the blood vessel feature is lost due to the folding effect.

To perform the recovery, we make use of all the pixels, i.e., $K + K' = P$. In addition, we

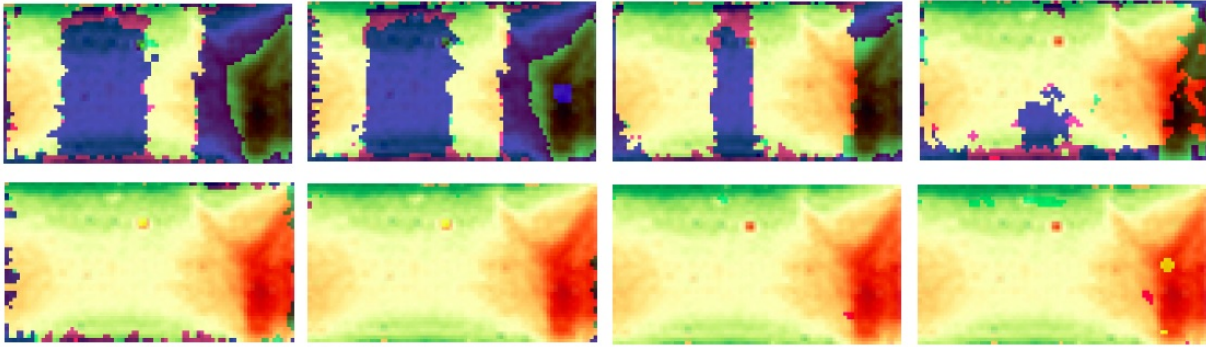


Fig. 11. The recovery results of the folded mouse brain surface image. Parameters from left to right and top to bottom: $\epsilon = 14\lambda, 16\lambda, \dots, 30\lambda$. Size of a $(\phi, \lambda/2 + \epsilon)$ -admissible partition: $0.33P, 0.34P, 0.21P, 0.20P, 0.14P, 0.076P, 0.054P, 0.032P$. Average recovery errors of the RGB channels: 36.7%, 37.0%, 18.0%, 11.0%, 2.61%, 0.41%, 0.13%, 0.74%.

assume unfolded observations are made at $\approx 0.05P$ pixels. We test extensively with different ϵ values in forming $(\phi, \lambda/2 + \epsilon)$ -admissible partitions of V . The recovery results are shown in Fig. 11. We see that as ϵ increases the size of a $(\phi, \lambda/2 + \epsilon)$ -admissible partition decreases, while the recovery performance increases initially. Moreover, when the partition size becomes too small, the performance starts to drop again. For all the four recovered images at the bottom, the blood vessel feature can be seen clearly.

We perform two additional sets of experiments on (compressed versions of) colored photo images.¹ Let p_{\max} be the maximum pixel value. For both images, we choose $\lambda = 0.7p_{\max}$. The folded images have severe color distortion (Fig. 12). We show the recovery results with $\epsilon = 16\lambda, 18\lambda, 20\lambda, 22\lambda, 24\lambda, 26\lambda$ in Fig. 12.

As observed before in the other experiments, for each image, the recovery performance first improves as ϵ increases and then drops. We may fuse the results for the 6 recovered images by taking a simple *majority voting* of the folding numbers. The fused images are also shown in Fig. 12, and we see that they give good recovery of the original images.

VI. CONCLUSION

In this paper, we study a spatio-temporal sampling approach for graph signals while considering a practical scenario of modulo-based sampling using self-reset ADC for high dynamic range signals. A theoretical graph sampling rate for recovery from folded signals has been provided,

¹Photos with ID 0030 and 0044 of <http://data.csail.mit.edu/graphics/fivek/>.

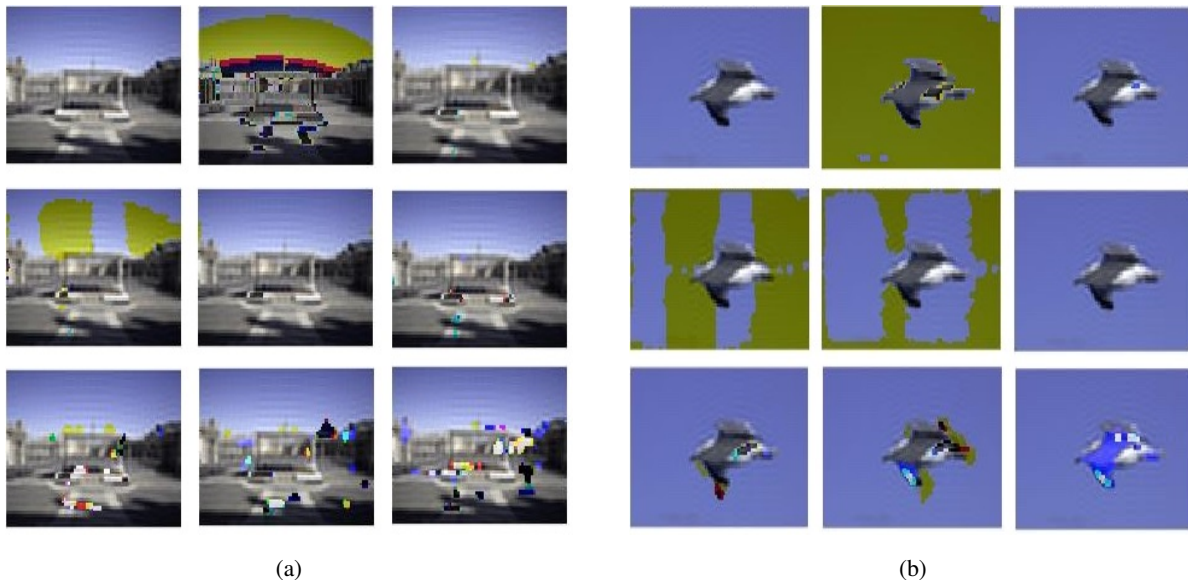


Fig. 12. Row 1: the original image, the folded image, and the recovered image by majority voting. Rows 2 and 3: recovered images with $\epsilon = 16\lambda, 18\lambda, 20\lambda, 22\lambda, 24\lambda, 26\lambda$, respectively.

which requires only the Nyquist-Shannon rate in the time direction. However, unconditional perfect recovery requires integer programming, which is intractable for large graphs. Under certain smoothness assumptions on the signals, we propose a new graph sampling scheme that minimize certain complexity measure introduced in the paper. Simulation results have been provided to demonstrate the performance of the proposed approach.

For future work, it is of interest to investigate improvement of our approach to make it more robust when the signal has large components in the high frequency regime.

APPENDIX A

GRAPHS WITH RANDOM EDGE WEIGHTS

In this appendix, we consider graphs with random edge weights, and demonstrate that several conditions being assumed in Theorem 1 and other places of the paper are common in this probabilistic setting.

Let $G = (V, E)$ be an undirected graph of size $n = |V|$. The edges in E are used to denote topological connections between pairs of nodes, and does not carry any metric information. We assign random weights to edges in E . More precisely, for each $e \in E$, let its weight a_e be a positive number chosen randomly according to a probability distribution absolutely continuous w.r.t. the Lebesgue measure. The weights are drawn independently for different edges. G coupled

with A , the associated weighted adjacency matrix, is called a *weighted model* of G . As the explicit choice of the probability distributions does not play a role in the discussion, we suppress them in the discussion.

We say that a property P *holds generally for G* if it holds for weighted models of G with probability one. A obviously weaker version is that P holds for at least one weighted model of G . We are interested in a property that holds generally for G as long as it holds for at least one weighted model.

For a weighted model (G, A) , let L be its weighted Laplacian matrix. Fix a positive integer $K \leq n$, a subset $S \subset V$ of size K and a node $u \in V \setminus S$ in case $K < n$. Arrange the eigenvalues $\lambda_1 \leq \dots \leq \lambda_n$ of L in ascending order and let w_i be an eigenvector corresponding to λ_i such that $\{w_1, \dots, w_n\}$ forms an orthonormal basis, whose existence is guaranteed by the spectral theorem. The collection of the first K basis element is denoted by $W = \{w_1, \dots, w_K\}$. The matrix W_S and vector W_u are defined as in Section II.

We consider the following list of related properties:

(a) P_0 : $\lambda_1, \dots, \lambda_n$ are all distinct.

(b) P_1 : W_S is invertible.

Q_1 : For any K distinct orthonormal eigenvectors $W' = \{w'_1, \dots, w'_K\} \subset \{w_1, \dots, w_n\}$ of L , W'_S is invertible.

(c) P_2 : the entries of $W_u W_S^{-1}$ are linearly independent over \mathbb{Z} .

Q_2 : For any K distinct orthonormal eigenvectors $W' = \{w'_1, \dots, w'_K\} \subset \{w_1, \dots, w_n\}$ of L , the entries of $W'_u W'^{-1}_S$ are linearly independent over \mathbb{Z} .

(d) P_3 : $W_u W_S^{-1}$ contains an irrational entry.

Q_3 : For any K distinct orthonormal eigenvectors $W' = \{w'_1, \dots, w'_K\} \subset \{w_1, \dots, w_n\}$ of L , $W'_u W'^{-1}_S$ contains an irrational entry.

(e) P_4 : the union of 1 and entries of $W_u W_S^{-1}$ are linearly independent over \mathbb{Z} .

Q_4 : For any K distinct orthonormal eigenvectors $W' = \{w'_1, \dots, w'_K\} \subset \{w_1, \dots, w_n\}$ of L , the union of 1 and entries of $W'_u W'^{-1}_S$ are linearly independent over \mathbb{Z} .

In P_2, P_3, P_4 (resp. Q_2, Q_3, Q_4) we implicitly assume P_1 (resp. Q_1) holds correspondingly. It is clear that if all of these properties holds generally for G separately, a combination of them also holds generally for G . Moreover, if Q_i holds generally for G , as a special case, so does $P_i, i = 1, 2, 3, 4$. On the other hand, it is possible to have G such that some P_i does not hold for any model of G , e.g., P_0 does not hold if G is disconnected.

To prepare for the discussions, we briefly discuss some key concepts and ideas. Details can be found in standard text books on differentiable manifolds, e.g., [37]. Recall that a differentiable manifold (abbreviated as manifold) X of dimension n is a topological space such that: at every point of $x \in X$, there is an open neighborhood U_x identified with an open subset of \mathbb{R}^n via a map f_x . Notion of differentiability can thus be defined on $f_x(U_x)$. If U_x and U_y intersect, then they are glued together via the transition function $\psi_{x,y} = f_y \circ f_x^{-1} : f_x(U_x \cap U_y) \rightarrow f_y(U_x \cap U_y)$. These $\psi_{x,y}$ are differentiable. The tangent space T_x at any point $x \in X$ is an n -dimensional vector space. A differentiable map between two manifolds $X \rightarrow Y$ is called a diffeomorphism if it has a differentiable inverse.

An m -dimensional manifold Y is a submanifold of X if there is a one-to-one map $f : Y \rightarrow X$ that induces a non-singular linear transformations between tangent spaces at every $y \in Y$. We call $n - m$ the co-dimension of Y .

A general strategy for the proofs of results in the Appendix goes as follows. We shall first construct a manifold X parametrized by graph edge weights, usually such an X carries the Lebesgue measure. If Y is a closed submanifold with co-dimension at least 1, detectable by looking at the derivative (or Jacobian) of the defining conditions, then it has measure 0. Or if Y is the locus of analytic functions (e.g., polynomials), then it is either all of X or has measure 0. For example, the locus of a single non-zero polynomial is a finite union of submanifolds each of co-dimension at least 1, and the locus has 0 Lebesgue measure.

We separate the discussion of P_0 from the rest, as W may not be unique if P_0 fails.

Lemma 3. *If P_0 holds for at least one weighted model, then P_0 holds generally for G .*

Proof: For a square matrix M , let $P_M(x) = \det(xI - M)$ be its characteristic polynomial, where I is the identity matrix of the same size.

For a weighted model (G, A) , the weighted Laplacian matrix L is parametrized by the strict upper triangular entries of A , i.e., the random edge weights $\{a_e : e \in E\}$. Thus, $P_L(x)$ is a polynomial on the variables $\{a_e : e \in E\} \cup \{x\} \subset \mathbb{R}^{|E|+1}$. For a given $\{a_e : e \in E\}$, P_0 fails if and only if there exists an $x \in \mathbb{R}$ such that $P_L(x) = 0$ and $P'_L(x) = dP_L(x)/dx = 0$ are satisfied simultaneously. Denote the simultaneous solution set $\{a_e : e \in E\} \cup \{x\}$ to be X .

Let $\mathbb{R}_{\geq 0}^{|E|}$ be the coordinates of the variables $\{a_e : e \in E\}$. If $X \cap \mathbb{R}_{\geq 0}^{|E|}$ is of co-dimension at least 1 in $\mathbb{R}_{\geq 0}^{|E|}$, then it has zero Lebesgue measure and hence P_0 holds generally. Otherwise, $X \cap \mathbb{R}_{\geq 0}^{|E|} = \mathbb{R}_{\geq 0}^{|E|}$. This is impossible as we assume that P_0 holds for at least one weighted model

(G, A) . The lemma is now proved. ■

Now, we work under the assumption that P_0 holds generally for G . As a consequence, we do not have any ambiguity in defining W , W_S , and W_u .

Proposition 1. *Suppose P_0 holds generally for G . For any $i = 1, 2, 3, 4$, if Q_i holds for at least one weighted model, then Q_i holds generally for G . In particular, P_i holds generally for G .*

Proof: Let $X \cong \mathbb{R}_{\geq 0}^{|E|}$ be the manifold parametrized by the strict upper triangular entries of A . Denote the Lebesgue measure on X by μ . As we assume that P_0 holds generally for G , there is an open submanifold X_0 consisting of weighted models whose Laplacian L has no repeated eigenvalues and whose complement is of co-dimension at least 1.

On the submanifold X_0 , the Schur decomposition [38] defines a smooth map

$$\psi : X_0 \rightarrow \mathbb{R}^{n^2} \times \mathbb{R}^n, A \mapsto (P_A, D_A),$$

where $L = P_A D_A P_A^{-1}$ is the unique Schur (orthonormal) decomposition of L . One should take note that the diagonal entries of D_A does not necessarily correspond to the ascending arrangement of the eigenvalues of A . Let Y be the image of ψ . Then, $\psi : X_0 \rightarrow Y$ is a diffeomorphism, whose inverse is given by $(P, D) \mapsto P D P^{-1}$, which is a polynomial.

Q_1 : For K distinct indices I of $\{1, \dots, n\}$, let $W_I = \{w_i : i \in I\}$ (W_I also denotes the matrix whose columns are $w_i, i \in I$) and $W_{I,S}$ be the submatrix of W_I consisting of rows indexed by S . Its determinant p_I is a polynomial on the coordinates of $Y \subset \mathbb{R}^{n^2}$. If p_I is non-vanishing on Y , then we are done. Otherwise, as Q_1 holds for at least one weighted model, p_I is not the constant 0 polynomial. Therefore, the locus Z_I of points of $p_I = 0$ is a finite union of submanifolds of co-dimension at least 1 in Y , and consequently $\mu(\psi^{-1}(Z_I)) = 0$. Define $Y_1 = Y \setminus (\cup_I Z_I)$. It follows immediately that the inverse image of the complement of Y_1 has zero Lebesgue measure. On the other hand, for any weighted model does not satisfy Q_1 , its Laplacian matrix belongs to $X_0 \setminus \psi^{-1}(Y_1)$. Therefore, Q_1 holds generally for G .

Q_2 : Let $a = (a_1)_{1 \leq i \leq K} \in \mathbb{Z}^K \setminus \{0\}$ be a nonzero (column) vector and I be K distinct indices I of $\{1, \dots, n\}$. Denote the subset of Y_1 such that the polynomial $\det(W_{I,S})W_{I,u}W_{I,S}^{-1}a = 0$ by $Z_{I,a}$. Suppose Q_2 holds for some models of G . As above, $Z_{I,a}$ is a submanifold of co-dimension at least 1. Hence, $\psi^{-1}(Z_{I,a})$ has zero Lebesgue measure. As the collection $\psi(\{Z_{I,a}\})$ is countable, their union has zero measure. Therefore, Q_2 holds generally for G .

The remaining cases are similar, and we shall be brief.

Q_3 : Let r be a rational number, I be K distinct indices of $\{1, \dots, n\}$, and $\{e_1, \dots, e_K\}$ be the standard basis of \mathbb{R}^K . Denote the subset of Y_1 such that $\det(W_{I,S})(W_{I,u}W_{I,S}^{-1}e_i - r) = 0$ by $Z_{I,r,i}$. If Q_3 holds for some models of G , $\mu(\psi^{-1}(Z_{I,r,i})) = 0$ as above. On the other hand, Q_3 holds for a model of G if it does not belong to any of $\psi^{-1}(Z_{I,r,i})$, which is a countable collection. Therefore, Q_3 holds generally for G .

Q_4 : Let $a = (a_1)_{1 \leq i \leq K} \in \mathbb{Z}^K \setminus \{0\}$ be a nonzero (column) vector, I be K distinct indices I of $\{1, \dots, n\}$ and $b \in \mathbb{Z}$. Denote the subset of Y_1 such that $\det(W_{I,S})(W_{I,u}W_{I,S}^{-1}a + b) = 0$ by $Z_{I,a,b}$. If Q_4 holds for some models of G , $\mu(\psi^{-1}(Z_{I,a,b})) = 0$ as above. On the other hand, Q_4 holds for a model of G if it does not belong to any of $\psi^{-1}(Z_{I,a,b})$, which is a countable collection. Therefore, Q_4 holds generally for G . ■

We remark here that the same argument also works without any changes if we are able to find a model with possibly negative edge weights. This relaxation of condition can be convenient in some arguments.

Example 1. *We shall use general, abstract but non-constructive arguments below, although in certain special cases, one can also perform explicit calculations.*

(a) *Let G be the path graph on n nodes for $n \geq 2$. We claim that P_0 holds generally for G .*

Let L_n be the Laplacian matrix of G with weight 1 for each edge and K_n be the $n \times n$ matrix obtained from L_n by replacing the (n, n) entry of L_n (which is 1 in L_n) by 2.

We first show by induction that: (1) K_n does not have repeated eigenvalues; and (2) K_n and K_{n+1} do not have common eigenvalues. It is straightforward to verify directly that both claims hold for K_2 and K_3 . Let λ be an eigenvalue of K_{n-1} , i.e., $\det(K_{n-1} - \lambda I_{n-1}) = 0$, and I_n be the $n \times n$ identity matrix, $n \geq 4$. By the induction hypothesis, $\det(K_{n-2} - \lambda I_{n-2}) \neq 0$. Apply the Laplace formula of matrix determinant (expanded w.r.t. the last row), one obtains:

$$\begin{aligned} |\det(K_n - \lambda I_n)| &= |(2 - \lambda) \det(K_{n-1} - \lambda I_{n-1}) - (-1) \cdot \det(K_{n-2} - \lambda I_{n-2})| \\ &= |\det(K_{n-2} - \lambda I_{n-2})| \neq 0. \end{aligned}$$

Therefore, λ is not an eigenvalue of K_n and we have proved claim (2). Let $\lambda_1 \leq \dots \leq \lambda_n$ be the eigenvalues of K_n and $\delta_1 < \dots < \delta_{n-1}$ be the distinct eigenvalues (by the induction hypothesis) of K_{n-1} . As the top-left block of K_n is K_{n-1} , we may invoke the Cauchy interlacing theorem ([39]) to obtain

$$\lambda_1 \leq \delta_1 \leq \lambda_2 \leq \dots \leq \lambda_{n-1} \leq \delta_{n-1} \leq \lambda_n. \quad (18)$$

However, as we have proved that K_n and K_{n-1} have distinct eigenvalues, the inequalities in (18) are all strict. Therefore, $\lambda_1, \dots, \lambda_n$ are distinct and this proves claim (1). Using the same argument, one can show that each L_n has distinct eigenvalues based on the fact that each K_n has distinct eigenvalues. Therefore, P_0 holds generally for G by Lemma 3.

As a consequence, P_0 holds generally for any G that contains a path connecting all the nodes.

- (b) Let G be the complete (simple) graph on n nodes for $n > 2$. We claim that each $P_i, i = 0, \dots, 4$ holds generally for G . First of all, as the complete graph contains a path of all the nodes, P_0 holds generally for G by (a).

For the other statements, we want to apply Proposition 1 to produce example for each individual case. As mentioned above, we allow models with negative edge weights. The space of all such models X can thus be identified with $\mathbb{R}^{n(n-1)/2}$. The Schur decomposition of the Laplacian matrix defines a map $\psi : X \rightarrow O(n)$, where $O(n)$ is the group of orthogonal matrices. On the other hand, for $P \in O(n)$, it is in the image of ψ if and only if there is a non-zero diagonal matrix D such that $PDP^T \mathbf{1} = 0$, where $\mathbf{1}$ is the all 1 column vector. This holds if and only if the sum of at least one column of P is 0. Therefore, $\psi(X)$ is the union of loci of $z \in O(n)$ satisfying the linear relation $l_i(z) = 0$, where $l_i(z)$ is the sum of the i -th column.

Let x be a model in X such that its Laplacian matrix L_x does not have repeated eigenvalues. As in the proof of Lemma 3, there is an open neighborhood U_x of x such that

- (i) For each $y \in U_x$, L_y does not have repeated eigenvalues.
- (ii) $\psi(U_x)$ is an open subset of $\psi(X)$.

For demonstration purpose, we explain Q_2 holds for some models. The same reasoning applies to Q_1, Q_3, Q_4 as well. It can be verified (by computing on test vectors) that for any non-zero vector of integers $a \in \mathbb{Z}^K$, the polynomial (on the matrix entries) $\det(M_S)M_u M_S^{-1}a$ does not contain any of l_i as a factor; i.e., the loci of l_i and $\det(M_S)M_u M_S^{-1}a$ intersects transversally in $O(n)$. Therefore, $\psi(U_x)$, which is an open subset of $O(n)$ satisfying at least one l_i , contain enough points to avoid the countable union of $\det(M_S)M_u M_S^{-1}a = 0$. Therefore, Q_2 holds for some models, and consequently, P_2 holds generally for G .

REFERENCES

- [1] D. I. Shuman, S. K. Narang, P. Frossard, A. Ortega, and P. Vandergheynst, "The emerging field of signal processing on graphs: Extending high-dimensional data analysis to networks and other irregular domains," *IEEE Signal Process. Mag.*, vol. 30, no. 3, pp. 83–98, May 2013.
- [2] A. Sandryhaila and J. M. F. Moura, "Discrete signal processing on graphs," *IEEE Trans. Signal Process.*, vol. 61, no. 7, pp. 1644–1656, April 2013.
- [3] —, "Big data analysis with signal processing on graphs: Representation and processing of massive data sets with irregular structure," *IEEE Signal Process. Mag.*, vol. 31, no. 5, pp. 80–90, Sept 2014.
- [4] A. Gadde, A. Anis, and A. Ortega, "Active semi-supervised learning using sampling theory for graph signals," in *Proc. ACM SIGKDD Int. Conf. on Knowledge Discovery and Data Mining*, New York, NY, USA, 2014, pp. 492–501.
- [5] S. Chen, A. Sandryhaila, J. M. F. Moura, and J. Kovačević, "Signal recovery on graphs: Variation minimization," *IEEE Trans. Signal Process.*, vol. 63, no. 17, pp. 4609–4624, Sept 2015.
- [6] X. Dong, D. Thanou, P. Frossard, and P. Vandergheynst, "Learning Laplacian matrix in smooth graph signal representations," *IEEE Trans. Signal Process.*, vol. 64, no. 23, pp. 6160–6173, Dec 2016.
- [7] H. E. Egilmez, E. Pavez, and A. Ortega, "Graph learning from data under Laplacian and structural constraints," *IEEE J. Sel. Top. Signal Process.*, vol. 11, no. 6, pp. 825–841, Sept 2017.
- [8] A. Ortega, P. Frossard, J. Kovačević, J. M. F. Moura, and P. Vandergheynst, "Graph signal processing: Overview, challenges, and applications," *Proc. IEEE*, vol. 106, no. 5, pp. 808–828, May 2018.
- [9] F. Ji and W. P. Tay, "A Hilbert space theory of generalized graph signal processing," *IEEE Trans. Signal Process.*, vol. 67, no. 24, pp. 6188 – 6203, Dec. 2019.
- [10] S. Chen, R. Varma, A. Sandryhaila, and J. Kovačević, "Discrete signal processing on graphs: Sampling theory," *IEEE Trans. Signal Process.*, vol. 63, no. 24, pp. 6510–6523, Dec 2015.
- [11] M. Tsitsvero, S. Barbarossa, and P. D. Lorenzo, "Signals on graphs: Uncertainty principle and sampling," *IEEE Trans. Signal Process.*, vol. 64, no. 18, pp. 4845–4860, Sept 2016.
- [12] A. Anis, A. Gadde, and A. Ortega, "Efficient sampling set selection for bandlimited graph signals using graph spectral proxies," *IEEE Trans. Signal Process.*, vol. 64, no. 14, pp. 3775–3789, July 2016.
- [13] K. Qiu, X. Mao, X. Shen, X. Wang, T. Li, and Y. Gu, "Time-varying graph signal reconstruction," *IEEE J. Sel. Top. Signal Process.*, vol. 11, no. 6, pp. 870–883, Sept 2017.
- [14] D. Romero, M. Ma, and G. B. Giannakis, "Kernel-based reconstruction of graph signals," *IEEE Trans. Signal Process.*, vol. 65, no. 3, pp. 764–778, Feb 2017.
- [15] F. Ji and W. P. Tay, "Generalized graph signal processing," in *Proc. IEEE Global Conf. on Signal and Information Processing*, Anaheim, USA, Nov. 2018.
- [16] Y. Tanaka, "Spectral domain sampling of graph signals," *IEEE Trans. Signal Process.*, vol. 66, no. 14, pp. 3752–3767, July 2018.
- [17] C. E. Shannon, "A mathematical theory of communication," *The Bell System Technical Journal*, vol. 27, no. 4, pp. 623–656, Oct 1948.
- [18] D. Park, J. Rhee, and Y. Joo, "A wide dynamic-range CMOS image sensor using self-reset technique," *IEEE Electron Device Letters*, vol. 28, no. 10, pp. 890–892, Oct 2007.
- [19] W. Kester, "ADC architectures VI: Folding ADCs (MT-025 tutorial)," Analog Devices, Tech. Rep., 2009.
- [20] W. Chou and R. M. Gray, "Modulo sigma-delta modulation," *IEEE Trans. Comm.*, vol. 40, no. 8, pp. 1388–1395, Aug 1992.

- [21] A. Bhandari, F. Kraemer, and R. Raskar, "On unlimited sampling," in *Int. Conf. Sampl. Theory and Appl.*, July 2017, pp. 31–35.
- [22] S. Rudresh, A. Adiga, B. A. Shenoy, and C. S. Seelamantula, "Wavelet-based reconstruction for unlimited sampling," in *IEEE Int. Conf. Acoustics, Speech and Signal Process.*, April 2018, pp. 4584–4588.
- [23] A. Bhandari, F. Kraemer, and R. Raskar, "Unlimited sampling of sparse signals," in *IEEE Int. Conf. Acoustics, Speech and Signal Process.*, April 2018, pp. 4569–4573.
- [24] Y. Chen, A. Basu, L. Liu, X. Zou, R. Rajkumar, G. Dawe, and M. Je, "A digitally assisted, signal folding neural recording amplifier," *IEEE Trans. Biomed. Circuits Syst.*, vol. 8, no. 4, pp. 528–542, Aug 2014.
- [25] O. Graf, A. Bhandari, and F. Kraemer, "One-bit unlimited sampling," in *IEEE Int. Conf. Acoustics, Speech and Signal Process.*, May 2019, pp. 5102–5106.
- [26] O. Musa, P. Jung, and N. Goertz, "Generalized approximate message passing for unlimited sampling of sparse signals," in *IEEE Global Conf. Signal and Information Proc.*, November 2018.
- [27] M. Cucuringu and H. Tyagi, "On denoising modulo 1 samples of a function," in *21st Intl. Conf. Artificial Intelligence and Statistics*, April 2018, pp. 1868–1876.
- [28] O. Ordentlich, G. Tabak, P. K. Hanumolu, A. C. Singer, and G. W. Wornell, "A modulo-based architecture for analog-to-digital conversion," *IEEE J. Sel. Top. Signal Process.*, vol. 12, no. 5, pp. 825–840, October 2018.
- [29] J. Cai, F. Ran, H. Yang, and M. Xu, "A CMOS image sensor with self-reset circuit in active pixel," in *Int. Cong. Image Signal Process.*, Oct 2009, pp. 1–4.
- [30] T. Yamaguchi, H. Takehara, Y. Sunaga, M. Haruta, M. Motoyama, Y. Ohta, T. Noda, K. Sasagawa, T. Tokuda, and J. Ohta, "Implantable self-reset CMOS image sensor and its application to hemodynamic response detection in living mouse brain," *Jpn. J. Appl. Phys.*, vol. 55, 04EM02, 2016.
- [31] F. Ji, Pratibha, and W. P. Tay, "On folded graph signals," in *Proc. IEEE Global Conf. on Signal and Information Processing*, Ottawa, Canada, Nov. 2019.
- [32] V. M. U. Feige and J. Vondrá, "Maximizing non-monotone submodular functions," in *Proc. 48th FOCS*, April 2007, pp. 461–471.
- [33] C. Shannon, "Communication in the presence of noise," *Proc. IRE*, vol. 86, pp. 10–21, 1949.
- [34] United States. Federal Energy Regulatory Commission North American Electric Reliability Corporation, "Arizona-southern california outages on september 8, 2011: Causes and recommendations," 2012.
- [35] R. Jethra, "Improving temperature measurement in power plants," *Power Engineering*, vol. 117, Mar. 2013.
- [36] W. Luo, W. P. Tay, and M. Leng, "Identifying infection sources and regions in large networks," *IEEE Trans. Signal Process.*, vol. 61, no. 11, pp. 2850–2865, 2013.
- [37] F. Warner, *Foundations of Differentiable Manifolds and Lie Groups*. New York: Springer, 1983.
- [38] L. Dieci and T. Eirola, "On smooth decompositions of matrices," *SIAM J. Matrix Anal. Appl.*, vol. 20, pp. 800–819, 1999.
- [39] S. G. Hwang, "Cauchy's interlace theorem for eigenvalues of hermitian matrices," *Amer. Math. Monthly*, vol. 111, no. 2, pp. 157–159, 2004.